Non-invasive detection of genomic imbalances in Hodgkin/ Reed-Sternberg cells in early and advanced stage Hodgkin's lymphoma by sequencing of circulating cell-free DNA: a technical proof-of-principle study

Peter Vandenberghe, Iwona Wlodarska, Thomas Tousseyn, Luc Dehaspe, Daan Dierickx, Magali Verheecke, Anne Uyttebroeck, Oliver Bechter, Michel Delforge, Vincent Vandecaveye, Nathalie Brison, Gregor E G Verhoef, Eric Legius, Frederic Amant, Joris R Vermeesch**

Summary

Background Hodgkin's lymphoma is one of the most common lymphoid neoplasms in young adults, but the low abundance of neoplastic Hodgkin/Reed-Sternberg cells in the tumour hampers the elucidation of its pathogenesis, biology, and diversity. After an incidental observation that genomic aberrations known to occur in Hodgkin's lymphoma were detectable in circulating cell-free DNA, this study was undertaken to investigate whether circulating cell-free DNA can be informative about genomic imbalances in Hodgkin's lymphoma.

Methods We applied massive parallel sequencing to circulating cell-free DNA in a prospective study of patients with biopsy proven nodular sclerosis Hodgkin's lymphoma. Genomic imbalances in Hodgkin/Reed-Sternberg cells were investigated by fluorescence in-situ hybridisation (FISH) on tumour specimens.

Findings By non-invasive prenatal testing (NIPT), we observed several genomic imbalances in circulating cell-free DNA of a pregnant woman, who was subsequently diagnosed with early-stage nodular sclerosis Hodgkin's lymphoma stage IIA during gestation. FISH on tumour tissue confirmed corresponding genomic imbalances in Hodgkin/Reed- Sternberg cells. We prospectively studied circulating cell-free DNA of nine nodular sclerosis Hodgkin's lymphoma cases: eight at first diagnosis and one at first relapse. Seven patients had stage IIA disease and two had stage IVB disease. In eight, genomic imbalances were detected, including, among others, gain of chromosomes 2p and 9p, known to occur in Hodgkin's lymphoma. These gains and losses in circulating cell-free DNA were extensively validated by FISH on Hodgkin/Reed-Sternberg cells in biopsy samples. Initiation of chemotherapy induced normalisation of circulating cell-free DNA profiles within 2–6 weeks. The cell cycle indicator Ki67 and cleaved caspase-3 were detected in Hodgkin/Reed-Sternberg cells by immunohistochemistry, suggesting high turnover of Hodgkin/Reed-Sternberg cells.

Interpretation In early and advanced stage nodular sclerosis Hodgkin's lymphoma, genomic imbalances in Hodgkin/ Reed-Sternberg cells can be identified by massive parallel sequencing of circulating cell-free DNA at diagnosis. The rapid normalisation of circulating cell-free DNA profiles on therapy initiation suggests a potential role for circulating cell-free DNA profiling in early response monitoring. This finding creates several new possibilities for exploring the diversity of Hodgkin's lymphoma, and has potential implications for the future clinical development of biomarkers and precision therapy for this malignancy.

Funding: KU Leuven - University of Leuven and University Hospitals Leuven.

Introduction

Hodgkin's lymphoma accounts for 11-30 % of all lymphomas and is the most common lymphoid neoplasm in adolescents and young adults. With the development of chemotherapy with or without radiotherapy in the past five decades, Hodgkin's lymphoma is highly curable today. However, 10-15% of patients will fail first-line therapy and will require salvage therapy, while a similar proportion is likely to be overtreated by first-line therapy.[1-3]

Remarkably, much of the therapeutic advances in Hodgkin's lymphoma took place without thorough knowledge of the origin and biology of the Hodgkin/Reed-Sternberg cell, the malignant cell in classical Hodgkin's lymphoma (classical Hodgkin's lymphoma). A salient feature of Hodgkin/Reed-Sternberg cells is their low abundance in biopsy samples, where they usually represent only 0·1-2% of the tumour mass, while the remainder is composed of a mixture of non-malignant immune cells. This has been a major obstacle in the study of the biology and genetics of classical Hodgkin's lymphoma, leading researchers to study Hodgkin/Reed-Sternberg cell-derived cell lines, or, more recently, Hodgkin/Reed-Sternberg cells captured by laser microdissection.[2-8]

In the past decade, the interest in circulating cell-free DNA has risen steeply in many medical disciplines.[9] The presence of fetal DNA fragments in plasma from pregnant women is the principle underlying non-invasive prenatal testing . Non-invasive prenatal testing is becoming widely implemented, either with assays targeting trisomies 13, 18 and 21, or by massive parallel sequencing, which also allows genome-wide detection of fetal aneuploidies and segmental imbalances [10]. In patients with cancer, circulating cell-free DNA may contain tumour-derived DNA, and hence be informative about the tumour genome. For instance, massive parallel sequencing on circulating cell-free DNA can reveal genome-wide tumour-associated copy number profiles.[11-13] In addition, Thierry and colleagues demonstrated that analysis of *KRAS* and *BRAF* mutation status on circulating cell-free DNA in metastatic colorectal cancer is highly specific and sensitive.[14] The analysis of circulating tumour DNA may also find other promising applications, such as early tumour detection, assessment of molecular disease heterogeneity, monitoring of response, detection of minimal residual disease, and molecular evolution and emergence of resistance.[9]

We recently implemented a novel non-invasive prenatal testing pipeline based on massive parallel sequencing of circulating cell-free DNA in pregnant women for prenatal testing[15]. The discovery of a patient with a complex circulating cell-free DNA profile due to early stage nodular sclerosis Hodgkin's lymphoma led us to investigate whether circulating cell-free DNA would be a useful tool to study the genetics of the disease.

METHODS

Participants

Ten patients in total were included in this study. The first blood sample of patient unique patient number (UPN)01 was obtained in the context of non-invasive prenatal testing. Subsequent patients with nodula sclerosis Hodgkin's lymphoma were recruited between April 29 2014, and July 2, 2014, at the University

Hospital Leuven, in a prospective study that assessed the detection of genomic imbalances in nodular sclerosis Hodgkin's lymphoma in circulating cell-free DNA at diagnosis and during therapy. Patients included were aged older than 12 years, had nodular sclerosis Hodgkin's lymphoma at first diagnosis or at relapse, had available of biopsy materials (cytogenetic specimens, fresh frozen or formalin-fixed paraffin embedded sections), and absence of concomitant malignancies. The study was approved by the Institutional Review Board of the University Hospitals Leuven, Belgium (Belgian number B32220141013, Study S56534/ML10468, date of approval 29/04/2014), and all participants provided written informed consent.

Genomic representation profiling

Blood was obtained in Cell-Free DNA BCT tubes (Streck, Omaha, NE, USA), and circulating cell-free DNA extracted from 4–5 mL of plasma. Sequencing libraries were prepared with the TruSeq Chip Sample preparation kit (Illumina, San Diego, CA, USA), indexed, and analysed by multiplex sequencing across both lanes of an Illumina HiSeq2500 (fast mode producing 50 bp single- end reads in pools of 23–24 samples).

The sequence reads were aligned to the reference genome with the Burrows-Wheeler aligner, de-duplicated with Picard instrument, and realigned and recalibrated with Genome Analysis Toolkit (GATK). Reads were removed that match (suboptimally) at multiple locations, require mismatches or gaps in the alignment, or start in blacklisted regions taken from an in-house curated list of common polymorphic copy-number variants, collapsed repeats, DAC blacklisted regions generated for the Encyclopedia of DNA elements (ENCODE) project, and the undefined portion of the reference genome. Thus, a minimum of $7{\cdot}9\times10^6$ reads (mean $10{\cdot}3\times10^6$ were obtained, corresponding to a minimum of roughly $11{\cdot}3\times10^6$ raw reads (mean $14{\cdot}5\times10^6$).[15]

The aligned and filtered reads were counted as described. Normalisation was done with respect to the autosomes. We partitioned all autosomes into 50 kb bins, corrected the sequence counts with LOESS regression according to the bin GC content, and divided the result by the sum of autosomal sequence counts, yielding t bin GC-corrected genomic representations. These were aggregated per autosome and per window representing 1/10th partitions of the chromosome, for which the windows are shifting by 50 kb. *Z*-scores for the genomic representation were calculated with mean and SD of genomic representations values from a reference set of 100 normal samples (50 men [46,XY], 50 women [46,XX] pregnancies). *Z*-scores greater than 1·5 and less than –1·5 suggested gain or gain or loss, respectively,[15] (for detailed description and references see appendix pp 2–3)

Array comparative genomic hybridisation (aCGH) and FISH

aCGH was done with 60k CytoSure ISCA v2 microarray, and analysed with CytoSure Interpret Software

(Oxford Gene Technology OGT, Oxford, UK). FISH was done on fixed cells from cytogenetic cultures, or on 5 µm sections of FFPE or snap-frozen biopsies following standard procedures. Combined FISH/CD30 immunostaining was done on 5 µm sections from snap-frozen biopsies. FISH images were acquired with a fluorescence microscope with an Axiophot2 camera (Carl Zeiss Microscopy, Jena, Germany) and ISIS software (MetaSystems, Altlussheim, Germany). Detailed methods and DNA probes are described in the appendix pp 3–4.

Immunohistochemistry and imaging

FFPE tissue sections were stained automatically (DAKO, Carpinteria, CA, USA). Antibodies against Ki67 (MIB1, DAK0, Glostrup, Denmark) and against cleaved caspase-3 (Ab2302, Abcam, Cambridge Science Park, Boston, MA, USA) were used as ready to use or at 1:50 dilution, respectively. Two expert independent observers counted Hodgkin/Reed-Sternberg cells in five representative high-power fields each. The percentage of Ki67-positive Hodgkin/Reed-Sternberg cells was estimated by visual interpretation of the immunohistochemical stain taking into account the presence of Ki67-positive small lymphocytes and larger histiocytes, in correlation with the cellular detail and distribution of the corresponding haematoxylin-eosin stain, CD30 immunostain, and the blue counterstain.

Routine classical Hodgkin's lymphoma staging and follow-up imaging was with FDG-PET/CT (UPN01–03 and UPN06–10) or CT (UPN04–05), or both.[16] During pregnancy, UPN01 was assessed by whole body diffusion- weighted MRI, a radiation and contrast medium free imaging modality (according to the protocols in clinical studies NCT00330447 and NCT01231269).[17]

Statistical analysis

Observed proportions and 95% exact (Clopper-Pearson) lower confidence limits are reported. Computations were done with the SAS, version 9.3.

Role of the funding source

The funders were not involved in the study design, data collection, data analysis, and data interpretation, or the writing of the report. All authors had full access to all of the data. PV had the final responsibility to submit for publication.

RESULTS

After analysis of more than 1000 cases with a recently implemented NIPT pipeline, a test on circulating cell-free DNA from a 27-year-old asymptomatic pregnant woman (UPN01) at 12-weeks gestational age yielded a markedly abnormal genomic representation profile. According to local

guidelines, a second circulating circulating cell-free DNA sample was obtained and analysed 2 weeks later with a similar result (figures 1, 2, appendix p 5), thus excluding poor quality of the sample and the sequencing process. Therefore, suspecting a biological reason for the aberrant profile, amniocentesis was done followed by aCGH and conventional karyotyping on amniotic cells: both indicated a normal diploid fetal genome (data not shown). The pregnant mother also had a normal diploid genome, as shown by aCGH on her lymphocytes (data not shown). Hence, a malignant disorder in mother or fetus, with somatically acquired genomic imbalances, was considered. A fetal tumour was excluded by expert fetal ultrasound, but whole body diffusion-MRI of the mother showed a confluent anterior mediastinal mass and several pathologically enlarged lymph nodes in the left lower cervical and bilateral retroclavicular regions, without involvement elsewhere. A CT-guided puncture biopsy of the mediastinal mass revealed a nodular sclerosis Hodgkin's lymphoma on pathological examination. aCGH on whole DNA from the biopsy sample showed a normal diploid pattern, as expected due to the rarity of Hodgkin/Reed-Sternberg cells (data not shown). Therefore, in search of genomic imbalances in Hodgkin/Reed-Sternberg cells, we [1] resorted to FISH analysis of FFPE biopsy sections. Three regions gained in the genomic representations profile, 8q terminal (ter), 9pter, and 14q, were examined with probes for *MYC* (8q24), *JAK2* (9p24), and *IGH* (14q32; [5] figure 1). The *JAK2* probe was applied together with a probe for centromere (CEP) 8, as ploidy control. Hodgkin/Reed-Sternberg cells showed three to four *MYC* signals, two CEP8 signals, one to two clusters of amplified *JAK2* signals in addition to two normal signals, [10] and four *IGH* signals (table). By contrast, normal patterns were noted in neighbouring cells (figure 1). Assuming a hyperdiploid status of Hodgkin/Reed-Sternberg cells in this case, the genomic gains in circulating cell-free DNA match with gains of the [15] corresponding chromosomal regions in Hodgkin/Reed- Sternberg cells, as shown by FISH. This strongly suggests that circulating cell-free DNA from UPN01 contains DNA representative of Hodgkin/Reed Sternberg cells. We hypothesised that aberrant genomic representation profiles in circulating cell-free DNA could be recurrent in nodular sclerosis Hodgkin's lymphoma. Therefore, circulating cell-free DNA was prospectively obtained from cases UPN02–10, consecutively diagnosed in our hospital with newly diagnosed nodular sclerosis Hodgkin's lymphoma (UPN02–04, UPN06–10) or with nodular sclerosis Hodgkin's lymphoma in first relapse (UPN05). Seven cases had supradiaphragmatic stage IIA disease and two had stage IVB disease (table).

Figure 2 shows a composite plot of the diagnostic genomic representations profiles of all patients, including UPN01. As in patient UPN01, the profiles of cases UPN03, UPN07, UPN08, UPN09, and UPN10 revealed substantial imbalances affecting several chromosomes or chromosomal arms, whereas in patients UPN04–06 fewer and less pronounced imbalances were noted. No obvious abnormalities were identified in patient UPN02 (figure 2) The most frequently affected regions, with gains seen in five or more patients, were 2p (n=7), 3q, 5p, and 9p/9pter (n=5). Other regions with gains in three or four patients included 8q/8qter, chromosome 12, and chromosome 19 (n=4), and 1q, 2q, 5q, chromosome 14, and 17q (n=3). Loss of 1p, 6q, 7q/qter, 9qter, 10q, 11qter, 13q, and 22q were noted in four or five patients, and loss of chromosome 4, 17p, chromosome 18 and 20p were each seen in three patients (figure 2).

To verify genomic representation profiles, all Hodgkin/ Reed-Sternberg cells that could be identified morphologically were extensively evaluated by FISH on cytogenetic specimens (table, figure 3). We noted a striking overall concordance between genomic imbalances in circulating cell-free DNA and altered copy numbers of the corresponding chromosomal regions in nearly all FISH experiments. For instance, the genomic representations profile of UPN08 indicated loss of 7q, nd gain of 1q, 2p, 7p, and 9p (excluding 9p24). These regions were explored by interphase FISH on cytogenetic specimens, with probes for *CKS1B* (1q21)/CEP1, *ALK* (2p23), *TCRG* (7p14)/CEP7, *D7S486* (7q31)/CEP7, and *JAK2* (9p24)/CEP8. Giant cells displayed three *CKS1B* signals versus two CEP1 signals, five to 11 signals for *ALK,* and three to four signals for *TCRG* versus two to three CEP7 signals. They also showed two to four signals. FISH thus confirmed gain of 1q, 2p, and 7p and loss of 7q (figure 3B– D, table). To identify the cells with abnormal hybridization patterns with certainty, we combined FISH for 2p24 *MYCN*) with CD30 immunostaining on the snap-frozen biopsy of UPN08. The giant cells with additional 2p24/ *MYCN* signals were CD30-positive, identifying them unequivocally as Hodgkin/Reed-Sternberg cells. Neighbouring cells with normal patterns were CD30- negative (figure 3F). Of note, the giant cells often displayed more than two centromeric signals for chromosomes 1, 7, or 8: this reflects the frequently polyploid and multinucleated state of Hodgkin/Reed- 15 Sternberg cells.[18] Additionally, several hybridisation patterns in the giant cells were often observed within experiments, consistent with the known subclonal variation of Hodgkin/Reed-Sternberg cells:[19] for instance, FISH for 9p24 in UPN08 showed a balanced pattern in 20 three cells and gain in three others, yielding only partial concordance with the genomic representations profile for 9p (figure 3E, table). The small surrounding non- malignant cells exhibited homogeneously normal hybridisation patterns.

FISH for *ALK* (2p23) indicated gain in UPN03–10, while UPN02 was confirmed to have two copies (table, figure 3G), consistent with genomic representations profiling in all but one case (UPN06). For *D7S486* (7q31), FISH and genomic representations profiling were concordant in all cases tested. For *JAK2* (9p24), FISH was in agreement with genomic representation profiling in UPN01–03 and UPN05–07. For UPN08–09, partial concordance was noted, again due to subclonal variation (table, figure 3A, G, H). UPN04 and UPN10 were discordant, with gain in FISH espite, respectively, a balance or loss in the genomic representations profile for 9p/9pter (table). Hence, with only three discordances in total, we noted a striking overall agreement between the genomic imbalances in circulating cell-free DNA by genomic representations profiling and those in Hodgkin/Reed-Sternberg cells identified by FISH. This cogently demonstrates that circulating cell-free DNA contains DNA derived from and representative of Hodgkin/Reed-Sternberg cells.

genomic representation profile aberrations were most pronounced in cases UPN08–09, each with stage IVB disease. This suggests a correlation between tumour load and Hodgkin/Reed-Sternberg cell-derived DNA in the circulating cell-free DNA. Nevertheless, genomic representation profiling also allowed detection of several aberrations in UPN03–07 and UPN10 with nodular sclerosis Hodgkin's lymphoma stage IIA, although some gains (2p23 in UPN06, and 9p24 in UPN04 and UPN10) were not correctly identified (table). Based on eight positive results out of nine prospectively recruited cases, the 95% ower limit for the proportion of positive samples equals 57%, implying strong evidence for abnormal circulating cell-free

DNA profiles in a substantial proportion of nodular sclerosis Hodgkin's lymphoma cases.

All patients, including the pregnant patient, were treated with combination doxorubicin, bleomycin, vinblastine, and dacarbazine chemotherapy with or without involved node radiotherapy, except UPN04–05 who were treated according to EuroNet-PHL recommendations. All responded as shown by early clinical evaluation. At the first interim PET/CT imaging evaluation after two to four cycles of chemotherapy, patients UPN01–04 and UPN06–10 all had reached complete metabolic remission. Patient UPN05 reached partial remission at the first interim evaluation by CT evaluation after four cycles and complete metabolic remission by PET and CT at the completion of chemotherapy. The abnormalities in the genomic representations profile at diagnosis were no longer observed in subsequent samples taken between day 15–43 after treatment initiation (figure 4, appendix p xx. This, in combination with the clinical disease response, further underscores the link between the abnormal genomic representations profiles and the malignant process and its burden. Furthermore, it suggests that early responses can be monitored non- invasively.

The ease by which Hodgkin/Reed-Sternberg DNA is detectable in circulating cell-free DNA contrasts with the paucity of Hodgkin/Reed-Sternberg cells in classical Hodgkin's lymphoma biopsies. We hypothesised that high Hodgkin/Reed-Sternberg cell turnover rates could be a key factor underlying this paradox. In general, Hodgkin/Reed-Sternberg cells showed bright nuclear expression of the cell cycle indicator Ki67 in all ten cases, with immunoreactivity ranging between 30–90% (median 80% [IQR 65–82]) of Hodgkin/Reed-Sternberg cells in individual patients. In addition to morphological signs of apoptosis, immunoreactivity with the anti- cleaved caspase-3 antibody was noted in a fraction of Hodgkin/Reed-Sternberg cells in six out of ten biopsies. Of note, areas of tissue necrosis were observed in two of the biopsies (figure 5).

Discussion

The scarcity of Hodgkin/Reed-Sternberg cells in classical Hodgkin's lymphoma biopsy samples has for a long time defied the identification of recurrent genetic lesions in classical Hodgkin's lymphoma, including nodular sclerosis Hodgkin's lymphoma.[2–8] Here, we report proof of-principle that genomic imbalances in Hodgkin/Reed- Sternberg cells can be profiled at diagnosis by massive parallel sequencing of circulating cell-free DNA in most cases with early and advanced stage nodular sclerosis Hodgkin's lymphoma. Of note, increased levels of circulating cell-free DNA were previously reported in classical Hodgkin's lymphoma, and correlated with unfavourable features. However, the origin of this circulating cell-free DNA was not further investigated.[20,21] This study is, to the best of our knowledge, the first to show that genomic imbalances of Hodgkin/Reed-Sternberg cells can be detected in circulating cell-free DNA (panel). The straightforward identification is unexpected but welcome, in that retrieving genetic information about Hodgkin/Reed- Sternberg cells from Hodgkin's lymphoma biopsy samples is notoriously demanding from a technical point of view. Indeed, the present knowledge

of the genetics of Hodgkin/Reed-Sternberg cells is almost entirely derived from a small number of studies of Hodgkin's lymphoma cell lines, and of microdissected Hodgkin/Reed- ternberg cells, after whole genome DNA amplification.[4–8] Reassuringly, the imbalances identified in this study of ten nodular sclerosis Hodgkin's lymphoma have previously been observed in aCGH studies on 1 microdissected Hodgkin/Reed-Sternberg cells, albeit with different frequencies.[4–8] Interestingly, we also confirm that 2p gain and 6q loss often occur together.[8] We also noted gain of 16p11–13, previously identified in 5 25% of classical Hodgkin's lymphoma, and associated with therapy resistance,[8] in two cases with stage IVB. The presence of informative amounts of Hodgkin/ Reed-Sternberg cell derived DNA in circulating cell-free DNA, despite their scarcity in classical Hodgkin's 10 lymphoma biopsy samples, probably implies that Hodgkin/Reed-Sternberg cells are subject to a higher cellular turnover rate than previously anticipated. Although we studied one proliferative and one apoptotic marker only, their coexpression on Hodgkin/Reed-Sternberg cells and the presence of necrosis in classical Hodgkin's lymphoma biopsy samples seem to support the notion that active proliferation is counterbalanced by high amounts of Hodgkin/Reed-Sternberg cell loss by apoptosis or necrosis, in keeping with expression studies 20 in Hodgkin/Reed-Sternberg cells.[22,23] This delicate balance might also explain the high efficacy of chemotherapy, because Hodgkin/Reed-Sternberg cells are already poised for cell death. genomic representations profiles were most greatly abnormal in in the two patients (UPN08–09) with advanced disease, suggesting an association between the Hodgkin/ Reed-Sternberg cell burden and the level of Hodgkin/ Reed-Sternberg cell derived DNA in circulating cell-free DNA. However, seven of eight patients with early stage IIA (including patient UPN01) had abnormal profiles too. On the basis of the high proportion of abnormal genomic representations profiles in this small series, a substantial, if not the major, proportion of cases with nodular sclerosis Hodgkin's lymphoma is expected to have abnormal circulating cell-free DNA profiles. Larger studies are needed to precisely determine the sensitivity of this technique in classical Hodgkin's lymphoma, in relation with the disease stage. These larger studies should also nclude the mixed cellularity, lymphocyte-rich, and lymphocyte-depleted subtypes of classical Hodgkin's lymphoma, and nodular lymphocyte predominant Hodgkin's lymphoma, less common types of Hodgkin's lymphoma, which were not included in this study.

The relation between the burden of Hodgkin/Reed- Sternberg cells and the abnormal genomic representation profiles is also underscored by the rapid clearance of genomic representation abnormalities present at diagnosis after the initiation of therapy. In view of this rapid clearance, genomic representation profiling seems 50 in the patterns of genomic imbalances. Again, larger unlikely to have great potential to sensitively monitor low levels of residual disease, even more so as it does not distinguish between reads from normal versus malignant Hodgkin/Reed-Sternberg cells. On the other hand, interim PET and CT is currently investigated as an instrument to guide therapeutic stratification in early response-adapted therapy.[24] Our findings suggest a potential for circulating cell-free DNA profiling in classical Hodgkin's lymphoma as a non-interventional instrument in staging and in early interim disease diagnostics as a first translational avenue.

Analysis of circulating cell-free DNA in Hodgkin's lymphoma might become a preferential gateway to

the genome of the Hodgkin/Reed-Sternberg cells because it circumvents the technical difficulty of purifying these cells from biopsies. Although the low resolution and coverage of genomic representations profiling restricts its potential for biological discovery or detection of point mutations, these limitations do not hold for other techniques applicable to circulating cell-free DNA.[9] Yet, the data from this series of ten patients suggest that genomic representation profiling can show heterogeneity in the patterns of genomic imbalances. Again, larger studies will be required to catalogue these patterns at diagnosis or relapse. This step will be highly relevant for translational research, as numerous signalling pathways can be deregulated in classical Hodgkin's lymphoma, including the NFκB and JAK-STAT pathways, with several of their players—eg, *REL* (2p16) and *JAK2* (9p24), affected by genomic gains.[2,6,8,25–28] Hence, genomic representation profiling of circulating cell-free DNA could open up several exciting possibilities—eg, to investigate prospectively whether specific genomic profiles are associated with responsiveness or resistance to conventional Hodgkin's lymphoma therapy,[7,8] or to explore genomic evolution of Hodgkin/Reed-Sternberg cells between initial diagnosis and relapse. Classical Hodgkin's lymphoma cell lines with 9p24/*JAK2* copy gain are sensitive to JAK2 inhibition in vitro and in vivo, suggesting that clinical trials of JAK2 blockade are warranted.[29] In this context, genomic representation profiling could be an attractive instrument to identify, in patients, the genomic patterns that predict the response to JAK2 inhibitors or other new biological agents. An additional asset of genomic representation profiling in such a context of pretherapy testing is its turn-around time of about 1 week. UPN01 exemplifies that concurrent malignancies with somatically acquired genomic imbalances can confound NIPT. This patient also represents, to the best of our knowledge, the first in whom such discordant NIPT results led to a diagnosis and treatment of malignancy during gestation. In another case with discordant NIPT results, a metastatic cancer was diagnosed only after at term delivery, with tumoural imbalances corresponding with the NIPT abnormalities.[30] Given a cancer incidence 25 of one per 1000–2000 person-years in 20–40-year-old women[31] and the present large-scale implementation of NIPT, one might wonder why no more cases have been reported to date. The NIPT focus on detection of fetal trisomies 13, 18, and 21 is a plausible reason,[10] but cancer 30 related variables could also be involved. The potential detection of some maternal cancers could be seen as an added value of NIPT and specific software adaptations to flag potential cancer related imbalances could be useful.

In conclusion, the presence of DNA derived from 35 Hodgkin/Reed-Sternberg cells in circulating cell-free DNA from classical Hodgkin's lymphoma patients opens important new perspectives for the exploration of the biology and for the diagnosis and management of early and advanced classical Hodgkin's lymphoma. Through facilitation of the development of long-awaited biomarkers and the design of clinical trials with novel biological drugs, this discovery might advance targeted and precision therapy in classical Hodgkin's lymphoma.

Contributors

PV, IW, EL, FA, and JRV conceived and designed the study. PV and IW designed and analysed FISH experiments. PV, IW, TT, DD, MV, AU, OB, MD, VV, GEGV, and FA included study patients and materials. LD and NB collected and assembled data. PV wrote the report with critical input from IW and JRV. All authors critically revised and approved the report.

Declaration of interests

We declare no competing interests

Acknowledgments

This trial was supported by research grants, from the KU Leuven (GOA/11/010 to PV, IW and TT; SymBioSys PFV/10/016 and GOA/12/015 to JRV), from the University Hospitals Leuven (Fund for Academic Studies to PV), from Research Fund-Flanders (FWO-Vlaanderen) (G081411N to TT), and from the Belgian Science Policy Office Interuniversity Attraction Poles (BELSPO-IAP) program through the project IAP P7/43-BeMGI. PV and FA are Senior Clinical Investigators of Research Fund-Flanders (FWO-Vlaanderen). MV is aspirant researcher of Research Fund-Flanders (FWO- Vlaanderen). TT holds a Mandate for Fundamental and Translational Research from the Stichting tegen Kanker. We thank Lucienne Michaux, Koen Devriendt, and Thomy de Ravel for critical reading; Geert Verbeke for statistical advice; Lode Danneels for patient referral; and Xavier Sagaert, Ursula Pluys, Julio Finalet Ferreiro, and Emilie Bittoun for assistance.

References

1 Stein H. Hodgkin Lymphoma. In: Swerdlow SH, Campo E, Harris NL, et al, eds. WHO Classification of Tumours of Haematopoietic and Lymphoid Tissues. Lyon: IARC; 2008.

2 Steidl C, Connors JM, Gascoyne RD. Molecular pathogenesis of Hodgkin's lymphoma: increasing evidence of the importance of the microenvironment. *J Clin Oncol* 2011; **29:** 1812–26.

3 Kuppers R, Engert A, Hansmann ML. Hodgkin lymphoma.*J Clin Invest* 2012; **122:** 3439–47.

4 Chui DT, Hammond D, Baird M, Shield L, Jackson R, Jarrett RF. Classical Hodgkin lymphoma is associated with frequent gains of 17q. *Genes Chromosomes Cancer* 2003; **38:** 126–36.

5 Hartmann S, Martin-Subero JI, Gesk S, et al. Detection of genomic imbalances in microdissected Hodgkin and Reed-Sternberg cells of classical Hodgkin's lymphoma by array-based comparative genomic hybridization. *Haematologica* 2008; **93:** 1318–26.

6 Joos S, Menz CK, Wrobel G, et al. Classical Hodgkin lymphoma is characterized by recurrent copy number gains of the short arm of chromosome 2. *Blood* 2002; **99:** 1381–87.

7 Slovak ML, Bedell V, Hsu YH, et al. Molecular karyotypes of Hodgkin and Reed-Sternberg cells at disease onset reveal distinct copy number alterations in chemosensitive versus refractory Hodgkin lymphoma. *Clin Cancer Res* 2011; **17:** 3443–54.

8 Steidl C, Telenius A, Shah SP, et al. Genome-wide copy number analysis of Hodgkin Reed-Sternberg cells identifies recurrent imbalances with correlations to treatment outcome. *Blood* 2010; **116:** 418–27.

9 Diaz LA Jr, Bardelli A. Liquid biopsies: genotyping circulating tumor DNA. *J Clin Oncol* 2014; **32:** 579–86.

10 Bianchi DW, Wilkins-Haug L. Integration of noninvasive DNA testing for aneuploidy into prenatal care: what has happened since the rubber met the road? *Clin Chem* 2014; **60:** 78–87.

11 Chan KC, Jiang P, Zheng YW, et al. Cancer genome scanning in plasma: detection of tumor-associated copy number aberrations, single-nucleotide variants, and tumoral heterogeneity by massively parallel sequencing. *Clin Chem* 2013; **59:** 211–24.

12 Heitzer E, Ulz P, Belic J, et al. Tumor-associated copy number changes in the circulation of patients with prostate cancer identified through whole-genome sequencing. *Genome Med* 2013; **5:** 30.

13 Leary RJ, Sausen M, Kinde I, et al. Detection of chromosomal alterations in the circulation of cancer patients with whole-genome sequencing. *Sci Transl Med* 2012; **4:** 162ra54.

14 Thierry AR, Mouliere F, El Messaoudi S, et al. Clinical validation of the detection of KRAS and BRAF mutations from circulating tumor DNA. *Nat Med* 2014; **20:** 430–35.

15 Bayindir B, Dehaspe L, Brison N, et al. Non-invasive Prenatal Testing (NIPT) using a novel analysis pipeline to screen for all autosomal fetal aneuploidies improves pregnancy

16 Cheson BD, Fisher RI, Barrington SF, et al. Recommendations for initial evaluation, staging, and response assessment of Hodgkin and Non-Hodgkin lymphoma: the Lugano classification. *J Clin Oncol* 2014; **32:** 3059–67.

17 Mayerhoefer ME, Karanikas G, Kletter K, et al. Evaluation of diffusion-weighted MRI for pretherapeutic assessment and staging of lymphoma: results of a prospective study in 140 patients. *Clin Cancer Res* 2014; **20:** 2984–93.

18 Rengstl B, Newrzela S, Heinrich T, et al. Incomplete cytokinesis and re-fusion of small mononucleated Hodgkin cells lead to giant multinucleated Reed-Sternberg cells. *Proc Natl Acad Sci USA* 2013; 110: 20729–34.

19 Weber-Matthiesen K, Deerberg J, Poetsch M, Grote W, Schlegelberger B. Numerical chromosome aberrations are present within the CD30+ Hodgkin and Reed-Sternberg cells in 100% of analyzed cases of Hodgkin's disease. *Blood* 1995; 86: 1464–68.

20 Hohaus S, Giachelia M, Massini G, et al. Cell-free circulating DNA in Hodgkin's and non-Hodgkin's lymphomas. *Ann Oncol* 2009; **20:** 1408–13.

21 Mussolin L, Burnelli R, Pillon M, et al. Plasma cell-free DNA in paediatric lymphomas. *J Cancer* 2013; **4:** 323–29.

22 Bai M, Papoudou-Bai A, Horianopoulos N, Grepi C, Agnantis NJ, Kanavaros P. Expression of bcl2 family proteins and active caspase 3 in classical Hodgkin's lymphomas. *Hum Pathol* 2007; **38:** 103–13.

23 Tiacci E, Doring C, Brune V, et al. Analyzing primary Hodgkin and Reed-Sternberg cells to capture the molecular and cellular pathogenesis of classical Hodgkin lymphoma. *Blood* 2012; **120:** 4609–20.

24 Gallamini A, Barrington SF, Biggi A, et al. The predictive role of interim positron emission tomography for Hodgkin lymphoma treatment outcome is confirmed using the interpretation criteria of the Deauville five-point scale. *Haematologica* 2014; **99:** 1107–13.

25 Martin-Subero JI, Gesk S, Harder L, et al. Recurrent involvement of the REL and BCL11A loci in classical Hodgkin lymphoma. *Blood* 2002; **99:** 1474–77.

26 Kato M, Sanada M, Kato I, et al. Frequent inactivation of A20 in B-cell lymphomas. *Nature* 2009; **459:** 712–16.

27 Green MR, Monti S, Rodig SJ, et al. Integrative analysis reveals selective 9p24.1 amplification, increased PD-1 ligand expression, and further induction via JAK2 in nodular sclerosing Hodgkin lymphoma and primary mediastinal large B-cell lymphoma. *Blood* 2010; **116:** 3268–77.

28 Van Roosbroeck K, Cox L, Tousseyn T, et al. JAK2 rearrangements,including the novel SEC31A-JAK2 fusion, are recurrent in classical Hodgkin lymphoma. *Blood* 2011; 117: 4056–64.

29 Hao Y, Chapuy B, Monti S, Sun HH, Rodig SJ, Shipp MA. Selective JAK2 inhibition specifically decreases Hodgkin lymphoma and mediastinal large B-cell lymphoma growth in vitro and in vivo. *Clin Cancer Res* 2014; 20: 2674–83.

30 Osborne CM, Hardisty E, Devers P, Kaiser-Rogers K, Hayden MA, Goodnight W, Vora NL. Discordant noninvasive prenatal testing results in a patient subsequently diagnosed with metastatic disease. *Prenat Diagn* 2013; 33: 609–11.

31 Ferlay J, Soerjomataram I, Ervik M, et al. Globocan 2012. Estimated cancer incidence, mortality and prevalence wordwide in 2012, 2014. http://globocan.iarc.fr/Pages/age-specific_table_sel.aspx (accessed Sept 29, 2014).

Blood was obtained in Cell-Free DNA BCT® tubes (Streck, Omaha, NE), and circulating cell-free DNA extracted from 4-5 ml of plasma. Sequencing libraries were prepared using the TruSeq Chip Sample preparation kit (Illumina, San Diego, CA), indexed and analyzed by multiplex sequencing across both lanes of an Illumina HiSeq2500 (fast mode producing 50bp single-end reads in pools of 23-24 samples).

The sequence reads were aligned to the reference genome using the Burrows-Wheeler aligner, de-duplicated with Picard tools (http://picard.sourceforge.net/), and realigned and recalibrated with GATK. Reads were removed that match (sub-optimally) at multiple locations, require mismatches or gaps in the alignment or start in blacklisted regions taken from an in-house curated list of common polymorphic CNV's, collapsed repeats, DAC blacklisted regions generated for the ENCODE project, and the undefined portion of the reference genome. Thus, minimum of $7{\cdot}9x10^6$ reads (mean $10{\cdot}3x10^6$) were obtained corresponding to a minimum of ~$11{\cdot}3x10^6$ raw reads (mean $14{\cdot}5\ x10^6$)[15].

The aligned and filtered reads were counted as described. Normalization was performed with respect to the autosomes. We partitioned all autosomes into 50-kb bins, corrected the sequence counts with LOESS regression according to the bin GC content, and divided the result by the sum of autosomal sequence counts, yielding bin GC-corrected genomic representations (GR). These were aggregated per autosome and per window representing $1/10^{th}$ partitions of the chromosome, where the windows are shifting by 50kb. Z-scores for the genomic representation were calculated using mean and standard deviation of genomic representation values from a reference set of 100 normal samples (50 male (46,XY), 50 female (46,XX) pregnancies). Z-scores >1·5 and <-1·5 suggest gain or loss respectively [15] (for detailed description and references see supplementary appendix).

Array comparative genomic hybridization (aCGH) and FISH

aCGH was performed with 60k CytoSure ISCA v2 microarray, and analyzed with CytoSure Interpret Software (Oxford Gene Technology OGT, Oxford, UK).

FISH was performed on fixed cells from cytogenetic cultures, or on 5 µm sections of FFPE or snap-frozen biopsies following standard procedures. Combined FISH/CD30 immunostaining was done on 5 µm sections from snap-frozen biopsies. FISH images were acquired with a fluorescence microscope with an Axiophot2 camera (Carl Zeiss Microscopy, Jena, Germany) and ISIS software (MetaSystems, Altlussheim, Germany). Detailed methods and DNA probes are described in the Supplementary Methods and Table S1.

Immunohistochemistry

FFPE tissue sections were stained automatically (DAKO, Carpinteria, CA). Antibodies against Ki67 (MIB1, DAK0, Glostrup, Denmark) and against cleaved caspase-3 (Ab2302, Abcam, Cambridge Science Park, Boston) were used as ready to use or at 1/50 dilution respectively. Two expert independent observers counted Hodgkin/Reed-Sternberg cells in five representative high power fields each. The percentage of Ki67 positive Hodgkin/Reed-Sternberg cells was estimated by visual interpretation of the immunohistochemical stain taking into account the presence of Ki67+ small lymphocytes and larger histiocytes, in correlation with the cellular detail and distribution of the corresponding HE stain, CD30 immunostain and the blue counterstain.

Imaging

Routine classical Hodgkin's lymphoma staging and follow-up imaging was with FDG-PET/CT (UPN01-03, UPN06-10) and/or CT (UPN04-05)[16]. During pregnancy, UPN01 was evaluated by whole body diffusion-weighted magnetic resonance imaging, a radiation and contrast medium free imaging modality (clinical studies NCT00330447 and NCT01231269).[17]

Statistical Analysis

Observed proportions and 95% exact (Clopper-Pearson) lower confidence limits are reported. Computations have been performed using the SAS statistical software package, version 9.3.

Role of the funding source

The funding sources were not involved in the study design, collection, analysis and interpretation of the data, or the writing of the manuscript. All authors had full access to all of the data. PV had the final responsibility to submit for publication.

RESULTS

Case report

Non-invasive prenatal testing was performed on circulating cell-free DNA from a 27-year old asymptomatic pregnant woman UPN01 at 12 weeks gestational age and yielded a markedly abnormal genomic representation profile. According to local guidelines, a second circulating cell-free DNA sample was obtained and analyzed 2 weeks later with a similar result (Figures 1 and 2, Figure S1), thus excluding poor quality of the sample and/or the sequencing process. Therefore, suspecting a biological reason for the aberrant profile, amniocentesis was performed followed by aCGH and conventional karyotyping on amniotic cells: both indicated a normal diploid fetal genome (not shown). The pregnant mother also had a normal diploid genome, as evidenced by aCGH on her lymphocytes (not shown). Hence, a malignant disorder in mother or fetus, with somatically acquired genomic imbalances, was considered. A fetal tumour was excluded by expert fetal ultrasound, but whole body diffusion-weighted magnetic resonance imaging of the mother showed a confluent anterior mediastinal mass and multiple pathologically enlarged lymph nodes in the left lower cervical and bilateral retroclavicular regions, without involvement elsewhere. A CT-guided puncture biopsy of the mediastinal mass revealed a NSHodgkin’s lymphoma on pathological examination. aCGH on whole DNA from the biopsy showed a normal diploid pattern, as expected (not shown). Therefore, in search of genomic imbalances in Hodgkin/Reed-Sternberg cells, we resorted to FISH analysis of FFPE biopsy sections. Three regions gained in the genomic representation profile, 8qter, 9pter and 14q,

were examined with probes for *MYC* (8q24), *JAK2* (9p24) and *IGH@* (14q32) (Figure 1). The *JAK2* probe was applied together with a probe for centromere (CEP) 8, as ploidy control. Hodgkin/Reed-Sternberg cells showed 3-4 *MYC* signals, two CEP8 signals, 1-2 clusters of amplified *JAK2* signals in addition to two normal signals, and four *IGH* signals (Table 1). In contrast, normal patterns were observed in neighbouring cells (Figure 1). Assuming a hyperdiploid status of Hodgkin/Reed-Sternberg cells in this case, the genomic gains in circulating cell-free DNA match with gains of the corresponding chromosomal regions in Hodgkin/Reed-Sternberg cells, as shown by FISH. This strongly suggests that circulating cell-free DNA from UPN01 contains DNA representative of Hodgkin/Reed-Sternberg cells.

Genomic representation profiling of circulating cell-free DNA recurrently reveals genomic imbalances in NSHodgkin's lymphoma

We hypothesized that aberrant genomic representation profiles in circulating cell-free DNA could be recurrent in NSHodgkin's lymphoma. Therefore, circulating cell-free DNA was prospectively obtained from cases UPN02-10, consecutively diagnosed in our hospital with newly diagnosed NSHodgkin's lymphoma (UPN02-04, UPN06-10) or with NSHodgkin's lymphoma in first relapse (UPN05). Seven cases had supradiaphragmatic stage IIA disease and two had stage IVB disease (Table 1).

Figure 2 shows a composite plot of the diagnostic genomic representation profiles of all patients, including UPN01. As in case UPN01, the profiles of cases UPN03, UPN07, UPN08, UPN09 and UPN10 revealed marked imbalances affecting several chromosomes or chromosomal arms, while in cases UPN04-06 fewer and less pronounced imbalances were found. No obvious abnormalities were identified in case UPN02 (Figure 2, Figure S1). The most frequently affected regions, with gain in five or more cases, were 2p (n=7), 3q, 5p and 9p/9pter (n=5). Other regions with gain in 3-4 cases included 8q/8qter, chromosome 12, and chromosome 19 (n=4), and 1q, 2q, 5q, chromosome 14, and 17q (n=3). Loss of 1p, 6q, 7q/qter, 9qter, 10q, 11qter, 13q and 22q were found in 4-5 cases, and loss of chromosome 4, 17p, chromosome 18 and 20p were each seen in three cases (Figure 2, Figure S1).

To verify genomic representation profiles, all Hodgkin/Reed-Sternberg cells that could be identified morphologically were extensively evaluated by FISH on cytogenetic specimens (Table 1, Figure 3). There was a striking overall concordance between genomic imbalances in circulating cell-free DNA and altered copy numbers of the corresponding chromosomal regions in nearly all FISH experiments. For instance, the genomic representation profile of UPN08 indicated loss of 7q, and gain of 1q, 2p, 7p, and 9p (excluding 9p24). These regions were explored by interphase FISH on cytogenetic specimens, using probes for *CKS1B* (1q21)/CEP1, *ALK* (2p23), *TCRG@* (7p14)/CEP7, *D7S486* (7q31)/CEP7, and *JAK2* (9p24)/CEP8. Giant cells displayed 3 *CKS1B* signals versus 2 CEP1 signals, 5-11 signals for *ALK,* and 3-4 signals for *TCRG@* versus 2-3 CEP7 signals. They also showed 2-4 signals for *D7S486* versus 4-8 CEP7 signals. FISH thus confirmed gain of 1q, 2p and 7p and loss of 7q (Figure 3B-D and Table 1). To identify the cells with abnormal hybridization patterns with certainty, we combined FISH for 2p24 (*MYCN*) with CD30 immunostaining on the snap-frozen biopsy of UPN08. The giant cells with additional 2p24/*MYCN* signals were CD30-positive, identifying them unequivocally as Hodgkin/Reed-Sternberg cells. Neighbouring cells with normal patterns were CD30-negative (Figure 3F). Of note, the giant cells often displayed more than two centromeric signals for chromosomes 1, 7 or 8: this reflects the frequently polyploid and multinucleated state of Hodgkin/Reed-Sternberg cells [18]. In addition, several hybridization patterns in the giant cells were often observed within experiments, consistent with the known subclonal variation of Hodgkin/Reed-Sternberg cells [19]: for instance, FISH for 9p24 in UPN08 showed a balanced pattern in three cells and gain in three others, yielding only partial concordance with the genomic representation profile for 9p (Figure 3E and Table 1). The small surrounding non-malignant cells exhibited homogeneously normal hybridisation patterns.

FISH for *ALK* (2p23) indicated gain in UPN03-10, while UPN02 was confirmed to have two copies (Table 1, Figure 3G), consistent with genomic representation profiling in all but one case (UPN06). For *D7S486 (*7q31), FISH and genomic representation profiling were concordant in all cases tested. For *JAK2* (9p24), FISH was in agreement with genomic representation profiling in UPN01-03 and UPN05-08. For UPN09, partial concordance was found, again due to

subclonal variation (Table 1, Figure 3A, G, H). UPN04 and UPN 10 were discordant, with gain in FISH despite, respectively, a balance or loss in the genomic representation profile for 9p/9pter (Table 1). Hence, with only three discordances in total, we find a striking overall agreement between the genomic imbalances in circulating cell-free DNA by genomic representation profiling and those in Hodgkin/Reed-Sternberg cells found by FISH. This cogently proves that circulating cell-free DNA contains DNA derived from and representative of Hodgkin/Reed-Sternberg cells.

genomic representation profile aberrations were most pronounced in cases UPN08-09, each with stage IVB disease. This suggests a correlation between tumour load and Hodgkin/Reed-Sternberg cell-derived DNA in the circulating cell-free DNA. Nevertheless, genomic representation profiling also allowed detection of several aberrations in UPN03-07 and UPN10 with NSHodgkin's lymphoma stage IIA, although some gains (2p23 in UPN06, and 9p24 in UPN04 and UPN10) were not correctly identified (Table 1). Based on eight positive results out of nine prospectively recruited cases, the 95% lower limit for the proportion of positive samples equals 57%: thus implying strong evidence for abnormal circulating cell-free DNA profiles in a considerable proportion of NSHodgkin's lymphoma cases.

Normal genomic representation profiles are restored upon initiation of antineoplastic therapy

All patients, including the pregnant patient, were treated with ABVD chemotherapy with or without involved node radiotherapy, except UPN04-05 who were treated according to EuroNet-PHodgkin's lymphoma recommendations. All responded as shown by early clinical evaluation. At the first interim PET/CT imaging evaluation after 2-4 cycles of chemotherapy, patients UPN01-04 and UPN06-10 all had reached complete metabolic remission. Patient UPN05 reached partial remission at the first interim evaluation by CT evaluation after 4 cycles and complete metabolic remission by PET/CT at the completion of chemotherapy. The abnormalities in the genomic representation profile at diagnosis were no longer observed in subsequent samples taken between day 15-43 after treatment initiation (Figure 4, Figure S2).

This, in combination with the clinical disease response, further underscores the link between the abnormal genomic representation profiles and the malignant process and its burden. Furthermore, it suggests that early responses can be monitored non-invasively.

Cell proliferation, apoptosis and necrosis in NSHodgkin's lymphoma

The ease by which Hodgkin/Reed-Sternberg DNA is detectable in circulating cell-free DNA contrasts with the paucity of Hodgkin/Reed-Sternberg cells in classical Hodgkin's lymphoma biopsies. We hypothesized that high Hodgkin/Reed-Sternberg turnover rates could be a key factor underlying this paradox. In general, Hodgkin/Reed-Sternberg cells showed bright nuclear expression of the cell cycle indicator Ki67 in all 10 cases, with immunoreactivity ranging between 30-90% (median 77%) of Hodgkin/Reed-Sternberg cells in individual cases. In addition to morphological signs of apoptosis, immunoreactivity with the anti-cleaved caspase-3 antibody was observed in a fraction of Hodgkin/Reed-Sternberg cells in 6/10 biopsies. Of note, areas of tissue necrosis were observed in two of 10 biopsies. Representative images are shown in Figure 5.

DISCUSSION

The scarcity of Hodgkin/Reed-Sternberg cells in classical Hodgkin's lymphoma biopsies has for a long time defied the identification of recurrent genetic lesions in classical Hodgkin's lymphoma, including NSHodgkin's lymphoma.[2-8] Here, we report proof-of-principle that genomic imbalances in Hodgkin/Reed-Sternberg cells can be profiled at diagnosis by massive parallel sequencing of circulating cell-free DNA in the majority of cases with early and advanced stage NSHodgkin's lymphoma.

Of note, elevated levels of circulating cell-free DNA were previously reported in classical Hodgkin's lymphoma, and correlated with unfavorable features. However, the origin of this circulating cell-free DNA was not further investigated[20,21]. This study is, to the best of our knowledge, the first to demonstrate that genomic imbalances of Hodgkin/Reed-Sternberg cells can be detected in circulating cell-free DNA. The straightforward identification in circulating cell-

free DNA of genomic imbalances in Hodgkin/Reed-Sternberg cells is unexpected but welcomed, in that retrieving genetic information on Hodgkin/Reed-Sternberg cells from Hodgkin's lymphoma biopsies is notoriously demanding from a technical point of view. Indeed, the current knowledge on the genetics of Hodgkin/Reed-Sternberg cells is almost entirely derived from a small number of studies of Hodgkin's lymphoma cell lines, and of microdissected Hodgkin/Reed-Sternberg cells, after whole genome DNA amplification[4-8]. Reassuringly, the imbalances identified in this study of ten NSHodgkin's lymphoma are already known from aCGH studies on microdissected Hodgkin/Reed-Sternberg cells, albeit with different frequencies.[4-8] Interestingly, we also confirm that 2p gain and 6q loss often occur together[8]. We also found gain of 16p11-13, previously identified in 25% of classical Hodgkin's lymphoma, and associated with therapy resistance[8], in two cases with stage IVB. The presence of informative amounts of Hodgkin/Reed-Sternberg cell derived DNA in circulating cell-free DNA, despite their scarcity in classical Hodgkin's lymphoma biopsies, probably implies that Hodgkin/Reed-Sternberg cells are subject to a higher cellular turnover rate than previously anticipated. Although we studied one proliferative and one apoptotic marker only, their coexpression on Hodgkin/Reed-Sternberg cells and the presence of necrosis in classical Hodgkin's lymphoma biopsies seem to support the notion that active proliferation is counterbalanced by high rates of Hodgkin/Reed-Sternberg cell loss by apoptosis or necrosis, in keeping with expression studies in Hodgkin/Reed-Sternberg cells.[22,23] This delicate balance might also explain the high cure rates of chemotherapy, as Hodgkin/Reed-Sternberg cells are already poised for cell death.

genomic representation profiles were most markedly abnormal in in the two patients (UPN08-09) with advanced disease, suggesting a correlation between the Hodgkin/Reed-Sternberg cell burden and the level of Hodgkin/Reed-Sternberg cell derived DNA in circulating cell-free DNA. However, seven of eight cases with early stage IIA (including patient UPN01) had abnormal profiles too. Based on the high proportion of abnormal genomic representation profiles in this small series, a substantial, if not the major, proportion of cases with NSHodgkin's lymphoma is expected to have abnormal circulating cell-free DNA profiles. Larger studies are needed to

precisely determine the sensitivity of this technique in classical Hodgkin's lymphoma, in relation with the disease stage. These larger studies should also include the mixed cellularity, lymphocyte-rich and lymphocyte-depleted subtypes of classical Hodgkin's lymphoma, and nodular lymphocyte predominant Hodgkin's lymphoma, less common types of Hodgkin's lymphoma which were not included in this study.

The relation between Hodgkin/Reed-Sternberg cell burden and the abnormal genomic representation profile is also underscored by the rapid clearance of genomic representation abnormalities present at diagnosis after the initiation of therapy. Given this rapid clearance, genomic representation profiling seems unlikely to have significant potential to sensitively monitor low levels of residual disease, even more so as it does not distinguish between reads from normal versus malignant Hodgkin/Reed-Sternberg cells. On the other hand, interim PET/CT is currently investigated as a tool guiding therapeutic stratification in early response-adapted therapy [24]. Our findings suggest a potential for circulating cell-free DNA profiling in classical Hodgkin's lymphoma as a non-interventional tool in staging and in early interim disease diagnostics as a first translational avenue.

Analysis of circulating cell-free DNA in Hodgkin's lymphoma might become a preferential gateway to the genome of the Hodgkin/Reed-Sternberg cells, as it circumvents the technical difficulty of purifying these cells from biopsies. While the low resolution and coverage of genomic representation profiling limit its potential for biological discovery or detection of point mutations, these limitations do not hold for other techniques applicable on circulating cell-free DNA [9]. Yet, the data from this series of ten patients suggest that genomic representation profiling can reveal heterogeneity in the patterns of genomic imbalances. Again, larger studies will be required to catalogue these patterns at diagnosis and/or relapse. This will be highly relevant for translational research, as numerous signaling pathways can be deregulated in classical Hodgkin's lymphoma, including the NFκB and JAK-STAT pathways, with several of their players, e.g. *REL* (2p16) and *JAK2* (9p24), affected by genomic gains [2,6,8,25-28]. Hence, genomic representation profiling of circulating cell-free DNA could open up several exciting possibilities, *e.g.* to investigate prospectively whether specific genomic profiles are indeed

associated with resistance to conventional Hodgkin's lymphoma therapy,[7,8] or to explore genomic evolution of Hodgkin/Reed-Sternberg cells between initial diagnosis and relapse. classical Hodgkin's lymphoma cell lines with 9p24/*JAK2* copy gain are sensitive to JAK2 inhibition *in vitro* and *in vivo,* suggesting that clinical trials of JAK2 blockade are warranted [29]. In this context, genomic representation profiling could be an attractive tool to identify, in patients, the genomic patterns that predict the response to JAK2 inhibitors or other new biological agents. An additional asset of genomic representation profiling in such a context of pretherapy testing is its turn-around-time of about one week.

UPN01 exemplifies that concurrent malignancies with somatically acquired genomic imbalances can confound Non-invasive prenatal testing. She also represents, to the best of our knowledge, the first patient in whom such discordant Non-invasive prenatal testing results led to a diagnosis and treatment of malignancy during gestation. In another case with discordant Non-invasive prenatal testing results, a metastatic cancer was diagnosed only after at term delivery, with tumoural imbalances corresponding with the Non-invasive prenatal testing abnormalities.[30] Given a cancer incidence of 1 per 1000-2000 person-years in 20-40 year old women[31] and the present large scale implementation of Non-invasive prenatal testing, one may wonder why no more cases have been reported to date. The Non-invasive prenatal testing focus on detection of fetal trisomies 13, 18 and 21 is a plausible reason,[10] but cancer related variables could also be involved. The potential detection of some maternal cancers could be seen as an added value of Non-invasive prenatal testing and specific software adaptations to flag potential cancer related imbalances could be useful.

In conclusion, the presence of DNA derived from Hodgkin/Reed-Sternberg cells in circulating cell-free DNA from classical Hodgkin's lymphoma patients opens important new perspectives for the exploration of the biology and for the diagnosis and management of early and advanced classical Hodgkin's lymphoma. Through facilitation of the development of long-awaited biomarkers and the design of clinical trials with novel biological agents, this discovery may advance targeted and precision therapy in classical Hodgkin's lymphoma.

CONTRIBUTORS

PV, IW, EL, FA and JRV conceived and designed the study. PV and IW designed and analysed FISH experiments. PV, IW, TT, DD, MV, AU, OB, MD, VV, GEGV and FA included study patients and materials. LD and NB collected and assembled data.

PV wrote the paper with critical input from IW and JRV. All authors critically revised and approved the manuscript. JRV and FA contributed equally.

CONFLICTS OF INTEREST

The authors declare no conflicts of interest.

ACKNOWLEDGMENTS

Supported by research grants, from the KU Leuven (GOA/11/010 to PV, IW and TT; SymBioSys PFV/10/016 and GOA/12/015 to JRV), from the University Hospitals Leuven (Fund for Academic Studies to PV), from Research Fund-Flanders (FWO-Vlaanderen) (G081411N to TT), and from the Belgian Science Policy Office Interuniversity Attraction Poles (BELSPO-IAP) program through the project IAP P7/43-BeMGI.

PV and FA are Senior Clinical Investigators of Research Fund-Flanders (FWO-Vlaanderen). MV is aspirant researcher of Research Fund-Flanders (FWO-Vlaanderen). TT holds a Mandate for Fundamental and Translational Research from the Stichting tegen Kanker.

We thank Prof. Lucienne Michaux and Prof Koen Devriendt for discussions; Prof. T. de Ravel for critical reading; Prof. G. Verbeke for statistical advice, dr. Lode Danneels for patient referral; and Ursula Pluys, Julio Finalet Ferreiro and Emilie Bittoun for excellent technical assistance.

REFERENCES

1. Stein H. Hodgkin Lymphoma. In: Swerdlow SH, Campo E, Harris NL, et al., eds. WHO Classification of Tumours of Haematopoietic and Lymphoid Tissues. Lyon: IARC; 2008: 332.

2. Steidl C, Connors JM, Gascoyne RD. Molecular pathogenesis of Hodgkin's lymphoma: increasing evidence of the importance of the microenvironment. *J Clin Oncol* 2011; **29**: 1812-26.

3. Kuppers R, Engert A, Hansmann ML. Hodgkin lymphoma. *J Clin Invest* 2012; **122**: 3439-47.

4. Chui DT, Hammond D, Baird M, Shield L, Jackson R, Jarrett RF. Classical Hodgkin lymphoma is associated with frequent gains of 17q. *Genes Chromosomes Cancer* 2003; **38**: 126-36.

5. Hartmann S, Martin-Subero JI, Gesk S, Husken J, Giefing M, Nagel I, Riemke J, Chott A, Klapper W, Parrens M, Merlio JP, Kuppers R, Brauninger A, Siebert R, Hansmann ML. Detection of genomic imbalances in microdissected Hodgkin and Reed-Sternberg cells of classical Hodgkin's lymphoma by array-based comparative genomic hybridization. *Haematologica* 2008; **93**: 1318-26.

6. Joos S, Menz CK, Wrobel G, Siebert R, Gesk S, Ohl S, Mechtersheimer G, Trumper L, Moller P, Lichter P, Barth TF. Classical Hodgkin lymphoma is characterized by recurrent copy number gains of the short arm of chromosome 2. *Blood* 2002; **99**: 1381-7.

7. Slovak ML, Bedell V, Hsu YH, Estrine DB, Nowak NJ, Delioukina ML, Weiss LM, Smith DD, Forman SJ. Molecular karyotypes of Hodgkin and Reed-Sternberg cells at disease onset reveal distinct copy number alterations in chemosensitive versus refractory Hodgkin lymphoma. *Clin Cancer Res* 2011; **17**: 3443-54.

8. Steidl C, Telenius A, Shah SP, Farinha P, Barclay L, Boyle M, Connors JM, Horsman DE, Gascoyne RD. Genome-wide copy number analysis of Hodgkin Reed-Sternberg cells identifies recurrent imbalances with correlations to treatment outcome. *Blood* 2010; **116**: 418-27.

9. Diaz LA, Jr., Bardelli A. Liquid biopsies: genotyping circulating tumour DNA. *J Clin Oncol* 2014; **32**: 579-86.

10. Bianchi DW, Wilkins-Haug L. Integration of noninvasive DNA testing for aneuploidy into prenatal care: what has happened since the rubber met the road? *Clin Chem* 2014; **60**: 78-87.

11. Chan KC, Jiang P, Zheng YW, Liao GJ, Sun H, Wong J, Siu SS, Chan WC, Chan SL, Chan AT, Lai PB, Chiu RW, Lo YM. Cancer genome scanning in plasma: detection of tumour-

associated copy number aberrations, single-nucleotide variants, and tumoural heterogeneity by massively parallel sequencing. *Clin Chem* 2013; **59**: 211-24.

12. Heitzer E, Ulz P, Belic J, Gutschi S, Quehenberger F, Fischereder K, Benezeder T, Auer M, Pischler C, Mannweiler S, Pichler M, Eisner F, Haeusler M, Riethdorf S, Pantel K, Samonigg H, Hoefler G, Augustin H, Geigl JB, Speicher MR. Tumor-associated copy number changes in the circulation of patients with prostate cancer identified through whole-genome sequencing. *Genome Med* 2013; **5**: 30.

13. Leary RJ, Sausen M, Kinde I, Papadopoulos N, Carpten JD, Craig D, O'Shaughnessy J, Kinzler KW, Parmigiani G, Vogelstein B, Diaz LA, Jr., Velculescu VE. Detection of chromosomal alterations in the circulation of cancer patients with whole-genome sequencing. *Sci Transl Med* 2012; **4**: 162ra54.

14. Thierry AR, Mouliere F, El Messaoudi S, Mollevi C, Lopez-Crapez E, Rolet F, Gillet B, Gongora C, Dechelotte P, Robert B, Del Rio M, Lamy PJ, Bibeau F, Nouaille M, Loriot V, Jarrousse AS, Molina F, Mathonnet M, Pezet D, Ychou M. Clinical validation of the detection of KRAS and BRAF mutations from circulating tumour DNA. *Nat Med* 2014; **20**: 430-5.

15. Bayindir B, Dehaspe L, Brison N, Brady P, Ardui S, Kamoun M, Van der Veken L, Lichtenbelt K, Van den Bogaert K, Van Houdt J, Zuffardi O, Van Esch H, De Ravel T, Legius E, Devriendt K, Vermeesch JR. Non-invasive Prenatal Testing using a novel analysis pipeline to screen for all autosomal fetal aneuploidies improves pregancy management.

16. Cheson BD, Fisher RI, Barrington SF, Cavalli F, Schwartz LH, Zucca E, Lister TA. Recommendations for Initial Evaluation, Staging, and Response Assessment of Hodgkin and Non-Hodgkin Lymphoma: The Lugano Classification. *J Clin Oncol* 2014; **32**: 3059-67.

17. Mayerhoefer ME, Karanikas G, Kletter K, Prosch H, Kiesewetter B, Skrabs C, Porpaczy E, Weber M, Pinker-Domenig K, Berzaczy D, Hoffmann M, Sillaber C, Jaeger U, Mullauer L, Simonitsch-Klupp I, Dolak W, Gaiger A, Ubl P, Lukas J, Raderer M. Evaluation of diffusion-weighted MRI for pretherapeutic assessment and staging of lymphoma: results of a prospective study in 140 patients. *Clin Cancer Res* 2014; **20**: 2984-93.

18. Rengstl B, Newrzela S, Heinrich T, Weiser C, Thalheimer FB, Schmid F, Warner K, Hartmann S, Schroeder T, Kuppers R, Rieger MA, Hansmann ML. Incomplete cytokinesis and re-fusion of small mononucleated Hodgkin cells lead to giant multinucleated Reed-Sternberg cells. *Proc Natl Acad Sci U S A* 2013; **110**: 20729-34.

19. Weber-Matthiesen K, Deerberg J, Poetsch M, Grote W, Schlegelberger B. Numerical chromosome aberrations are present within the CD30+ Hodgkin and Reed-Sternberg cells in 100% of analyzed cases of Hodgkin's disease. *Blood* 1995; **86**: 1464-8.

20. Hohaus S, Giachelia M, Massini G, Mansueto G, Vannata B, Bozzoli V, Criscuolo M, D'Alo F, Martini M, Larocca LM, Voso MT, Leone G. Cell-free circulating DNA in Hodgkin's and non-Hodgkin's lymphomas. *Ann Oncol* 2009; **20**: 1408-13.

21. Mussolin L, Burnelli R, Pillon M, Carraro E, Farruggia P, Todesco A, Mascarin M, Rosolen A. Plasma cell-free DNA in paediatric lymphomas. *J Cancer* 2013; **4**: 323-9.

22. Bai M, Papoudou-Bai A, Horianopoulos N, Grepi C, Agnantis NJ, Kanavaros P. Expression of bcl2 family proteins and active caspase 3 in classical Hodgkin's lymphomas. *Hum Pathol* 2007; **38**: 103-13.

23. Tiacci E, Doring C, Brune V, van Noesel CJ, Klapper W, Mechtersheimer G, Falini B, Kuppers R, Hansmann ML. Analyzing primary Hodgkin and Reed-Sternberg cells to capture the molecular and cellular pathogenesis of classical Hodgkin lymphoma. *Blood* 2012; **120**: 4609-20.

24. Gallamini A, Barrington SF, Biggi A, Chauvie S, Kostakoglu L, Gregianin M, Meignan M, Mikhaeel GN, Loft A, Zaucha JM, Seymour JF, Hofman MS, Rigacci L, Pulsoni A, Coleman M, Dann EJ, Trentin L, Casasnovas O, Rusconi C, Brice P, Bolis S, Viviani S, Salvi F, Luminari S, Hutchings M. The predictive role of interim positron emission tomography for Hodgkin lymphoma treatment outcome is confirmed using the interpretation criteria of the Deauville five-point scale. *Haematologica* 2014; **99**: 1107-13.

25. Martin-Subero JI, Gesk S, Harder L, Sonoki T, Tucker PW, Schlegelberger B, Grote W, Novo FJ, Calasanz MJ, Hansmann ML, Dyer MJ, Siebert R. Recurrent involvement of the REL and BCL11A loci in classical Hodgkin lymphoma. *Blood* 2002; **99**: 1474-7.

26. Kato M, Sanada M, Kato I, Sato Y, Takita J, Takeuchi K, Niwa A, Chen Y, Nakazaki K, Nomoto J, Asakura Y, Muto S, Tamura A, Iio M, Akatsuka Y, Hayashi Y, Mori H, Igarashi T, Kurokawa M, Chiba S, Mori S, Ishikawa Y, Okamoto K, Tobinai K, Nakagama H, Nakahata T, Yoshino T, Kobayashi Y, Ogawa S. Frequent inactivation of A20 in B-cell lymphomas. *Nature* 2009; **459**: 712-6.

27. Green MR, Monti S, Rodig SJ, Juszczynski P, Currie T, O'Donnell E, Chapuy B, Takeyama K, Neuberg D, Golub TR, Kutok JL, Shipp MA. Integrative analysis reveals selective 9p24.1 amplification, increased PD-1 ligand expression, and further induction via JAK2 in nodular sclerosing Hodgkin lymphoma and primary mediastinal large B-cell lymphoma. *Blood* 2010; **116**: 3268-77.

28. Van Roosbroeck K, Cox L, Tousseyn T, Lahortiga I, Gielen O, Cauwelier B, De Paepe P, Verhoef G, Marynen P, Vandenberghe P, De Wolf-Peeters C, Cools J, Wlodarska I. JAK2 rearrangements, including the novel SEC31A-JAK2 fusion, are recurrent in classical Hodgkin lymphoma. *Blood* 2011; **117**: 4056-64.

29. Hao Y, Chapuy B, Monti S, Sun HH, Rodig SJ, Shipp MA. Selective JAK2 inhibition specifically decreases Hodgkin lymphoma and mediastinal large B-cell lymphoma growth in vitro and in vivo. *Clin Cancer Res* 2014; **20**: 2674-83.

30. Osborne CM, Hardisty E, Devers P, Kaiser-Rogers K, Hayden MA, Goodnight W, Vora NL. Discordant noninvasive prenatal testing results in a patient subsequently diagnosed with metastatic disease. *Prenat Diagn* 2013; **33**: 609-11.

31. Ferlay J, Soerjomataram I, Ervik M, Forman D, Bray F, Dikshit R, Elser S, Mathers C, Rebelo M, Parkin DM. Globocan 2012. Estimated Cancer Incidence, Mortality and Prevalence Wordwide in 2012. 2014. http://globocan.iarc.fr/Pages/age-specific_table_sel.aspx (accessed September 29, 2014.

FIGURES AND FIGURE LEGENDS

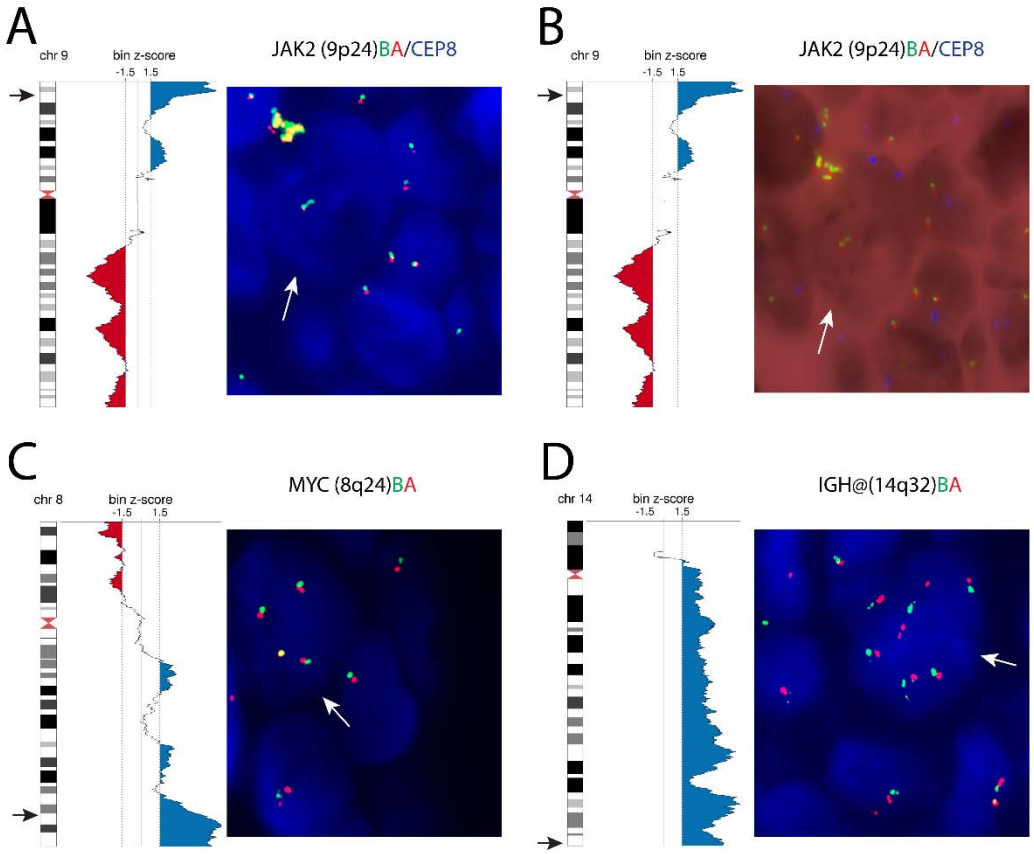

Figure 1. **genomic representation profile and FISH analysis of selected chromosomes of patient UPN01.**

The left of each panel shows a chromosomal genomic representation profile with z-scores (horizontal axis) in relation to the chromosomal position (vertical axis, aligned with the chromosomal idiogram). The area under the curve is shown in blue for z-scores > 1·5 (suggesting gain) and in red for z-scores <-1·5 (suggesting loss). On the right of each panel, representative FISH images of interphase nuclei, including one giant RS cell (white arrow) and several other small interphase cells, are shown. The arrow on the idiogram indicates the chromosomal location of the home-made or LSI probe used

A-B. Chromosome 9 with gain of 9p24 (arrow). FISH probes: home-made *JAK2* break-apart (red/green) (9p24) and CEP8 (blue). Both images were captured using a DAPI/FITC/SpectrumOrange/DEAC-band pass filter, but image B is shown in inverted gray scale to visualize blue (Spectrum Aqua) CEP8 signals.

C. Chromosome 8 with gain of 8q24 (arrow). FISH probe: LSI *MYC* break apart (red/green) (8q24)

D. Gain of chromosome 14 (arrow). FISH probe: LSI *IGH*@ break-apart (red/green) (14q32).

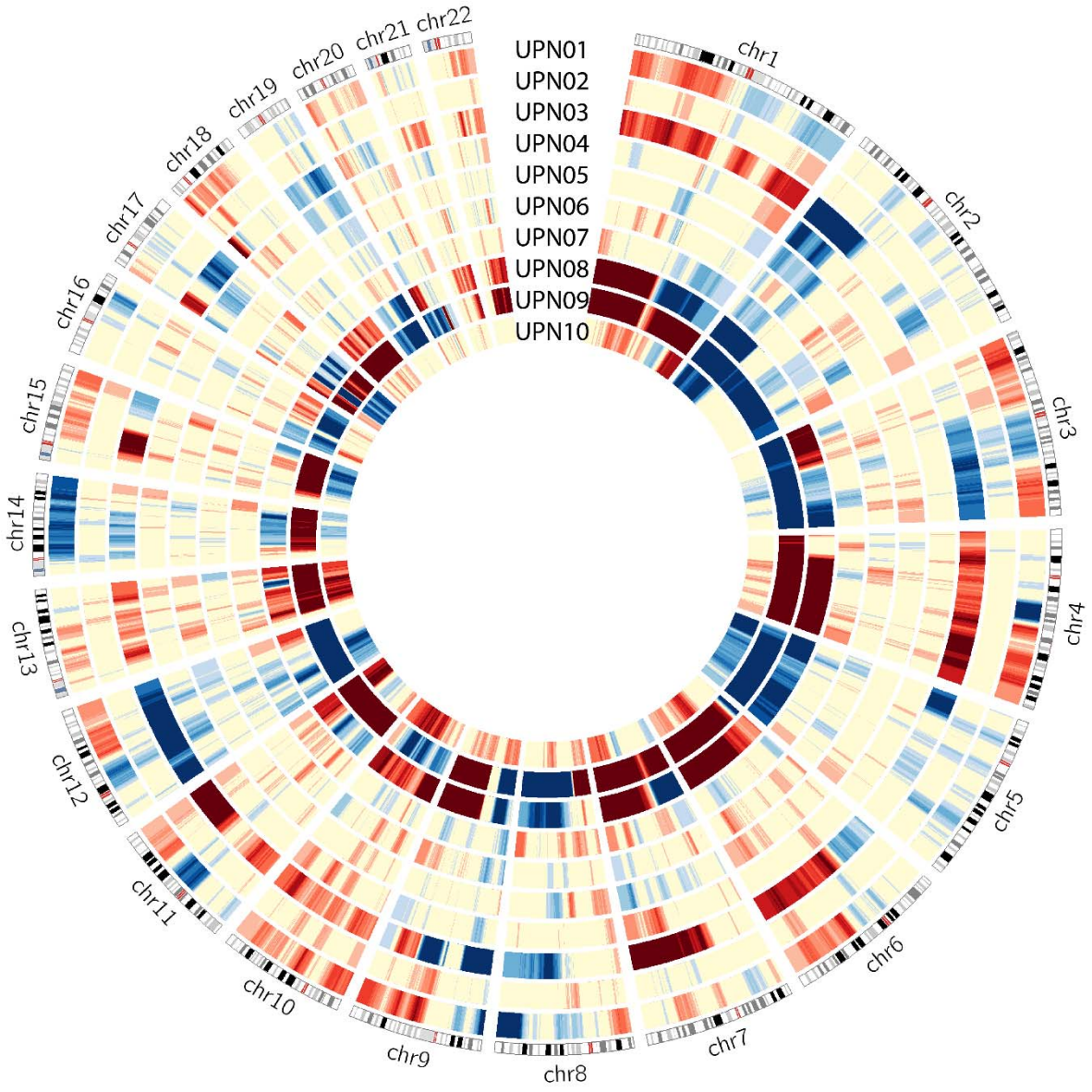

Figure 2. **genomic representation profiles of cases UPN01-10.**

The circos plot shows the genomic representation profile of the autosomal chromosomes in clockwise order, aligned with chromosomal idiograms (outer circle). UPN01-10 are shown from the periphery to the center. Z-scores >1·5 (suggesting gain) are shown in blue, and z-scores < -1·5 (suggesting loss) in red, where darker colors represent higher absolute values of z-scores. Z-scores between -1·5 and +1·5 are shown in yellow. Seven color grades are used to indicate six z-score intervals of length 0·75 ranging from 1·5 (-1·5) to 6 (-6). The seventh, darkest color is reserved for values >6 or <-6.

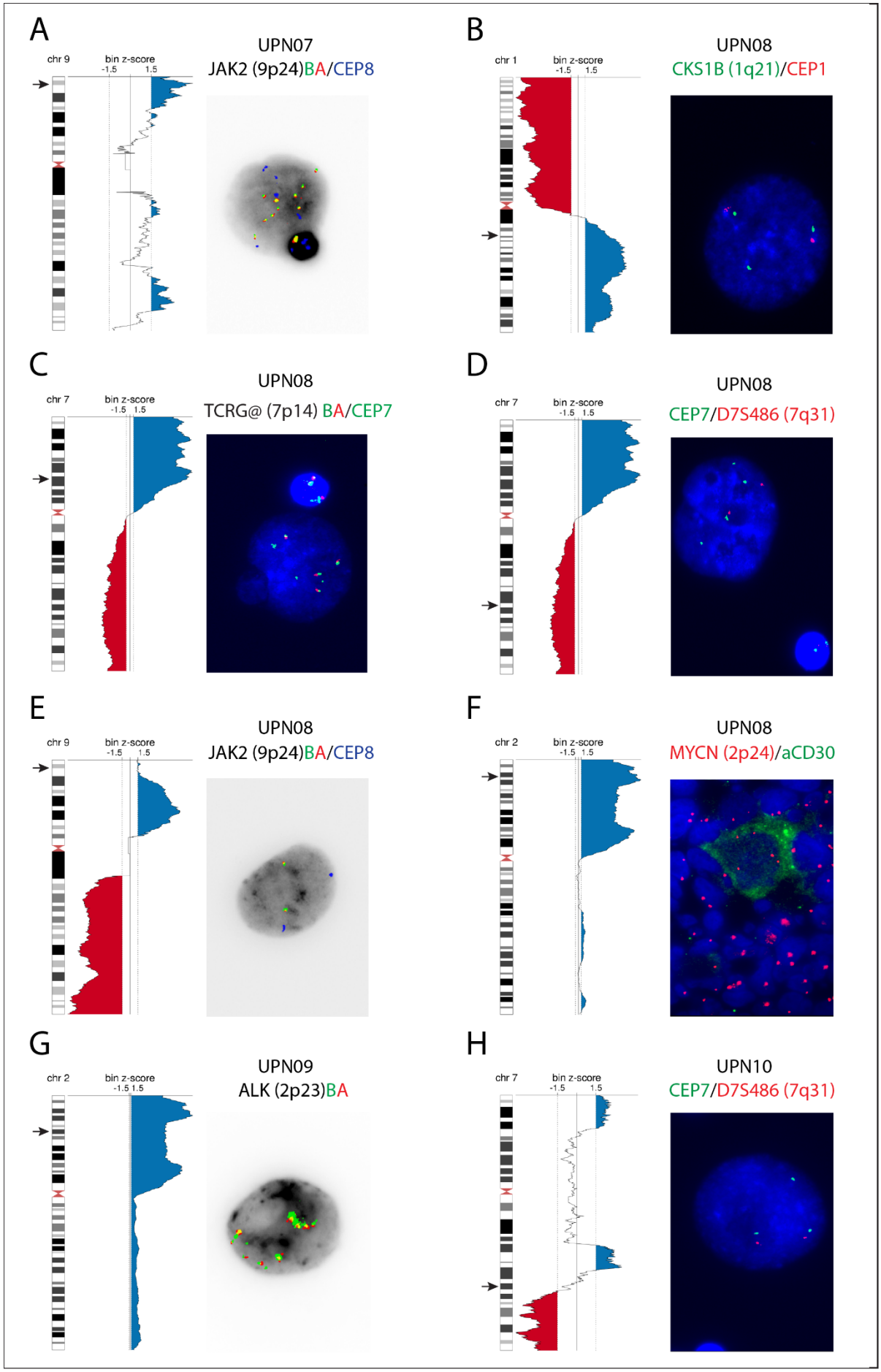
A
chr 9
bin z-score
-1.5
1.5
UPN07
JAK2 (9p24)BA/CEP8
B
chr 1
bin z-score
-1.5
1.5
UPN08
CKS1B (1q21)/CEP1
C
chr 7
bin z-score
-1.5
1.5
UPN08
TCRG@ (7p14) BA/CEP7
D
chr 7
bin z-score
-1.5
1.5
UPN08
CEP7/D7S486 (7q31)
E
chr 9
bin z-score
-1.5
1.5
UPN08
JAK2 (9p24)BA/CEP8
F
chr 2
bin z-score
-1.5
1.5
UPN08
MYCN (2p24)/aCD30
G
chr 2
bin z-score
-1.5
1.5
UPN09
ALK (2p23)BA
H
chr 7
bin z-score
-1.5
1.5
UPN10
CEP7/D7S486 (7q31)

Figure 3. **genomic representation profile and FISH analysis of selected chromosomes of patients UPN07-10.**

The genomic representation profile of selected chromosomes is shown at the left of each panel, aligned with the corresponding idiograms .The area under the curve is in blue for z-scores > 1·5 and in red for z-scores <-1·5. Note that the scale of the horizontal axis varies between patients. To the right of each panel, a representative interphase FISH image is shown. The arrow on the idiogram indicates the chromosomal location of homebrew or LSI probes used.

A. UPN07. genomic representation profile of chromosome 9. Interphase FISH image of a giant Hodgkin/Reed-Sternberg cell and a small non-Hodgkin/Reed-Sternberg cell, confirming amplification of *JAK2* (9p24) (red/green) in the giant cell relative to CEP8 (blue).

B. UPN08. genomic representation profile of chromosome 1. Interphase FISH image of a giant Hodgkin/Reed-Sternberg cell, confirming gain of *CKS1B* (1q21) (green) over CEP1 (red).

C. UPN 08. genomic representation profile of chromosome 7. Interphase FISH image of a giant Hodgkin/Reed-Sternberg cell and a small non-Hodgkin/Reed-Sternberg cell, confirming gain of *TCRG@* (7p14) (red/green) over CEP7 (green) in the Hodgkin/Reed-Sternberg cell.

D. UPN 08. genomic representation profile of chromosome 7. Interphase FISH image of a giant Hodgkin/Reed-Sternberg cell and a small non-Hodgkin/Reed-Sternberg cell confirming loss of *D7S486* (7q31) (red) relative to CEP7 (green) in the Hodgkin/Reed-Sternberg cell.

E. UPN08. genomic representation profile of chromosome 9, with gain of 9p, but not including 9p24 (arrow). Interphase FISH image of a giant Hodgkin/Reed-Sternberg cell with 2 signals for *JAK2* (9p24) (red/green) and centromere 8.

F. UPN08. genomic representation profile of chromosome 2. Image of combined FISH for *MYCN* (2p24) (red) and immunostaining for CD30 (green). The giant cell with 5 signals for *MYCN* is immunoreactive with anti-CD30, in contrast with the surrounding cells with two hybridization signals.

G. UPN09. GR profile of chromosome 2. Interphase FISH image of a giant Hodgkin/Reed-Sternberg cell with amplification of *ALK* (2p23) (red/green).

H. UPN10. genomic representation profile of chromosome 7. Interphase FISH image of a giant Hodgkin/Reed-Sternberg cell, confirming loss of *D7S486* (7q31) (red) relative to CEP7 (green).

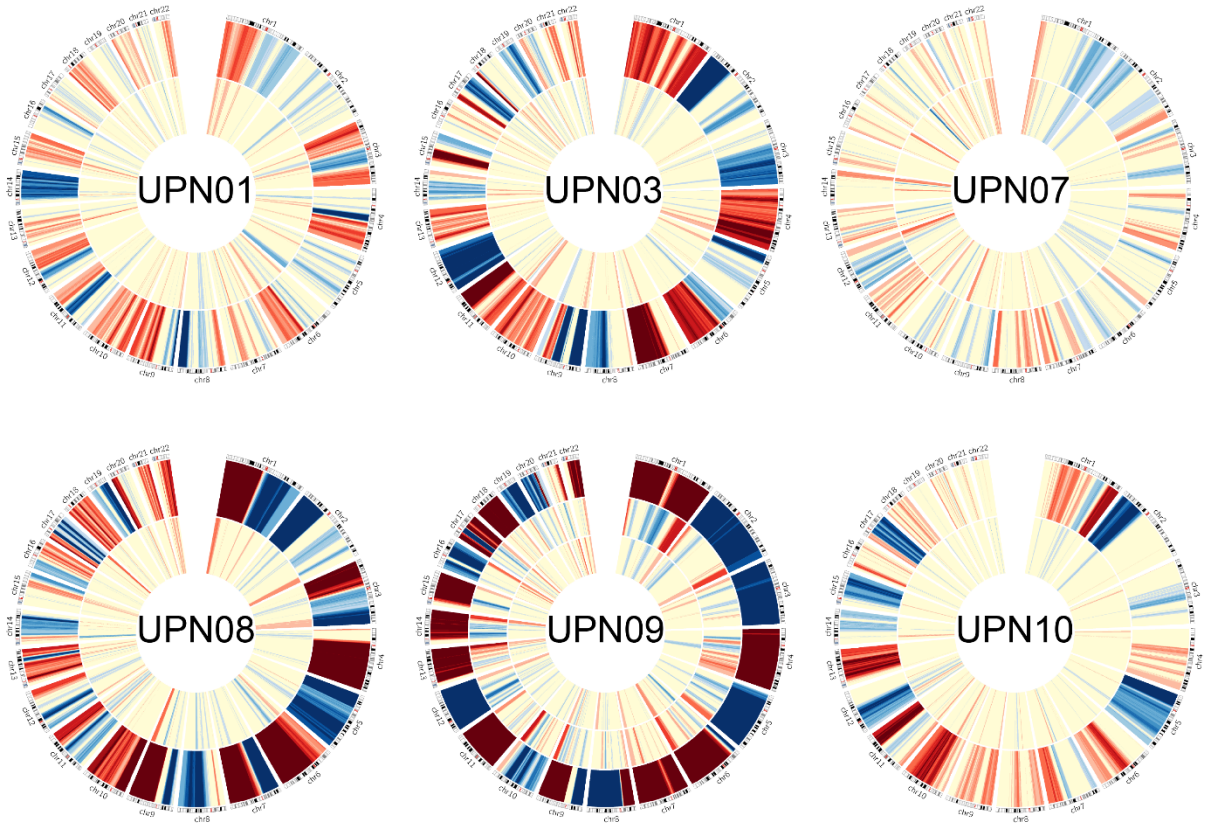

Figure 4. **genomic representation profiles before and after treatment initation.**

Circos plots show GR profiles of the autosomal chromosomes in clockwise order, aligned with chromosomal idiograms (outer circle), before therapy and after therapy initiation for UPN01, UPN03, UPN 07-10. The pretherapy genomic representation profile is shown as the outer circle, while the inner circle(s) show(s) genomic representation profiles after therapy initiation. The samples after treatment initiation were obtained at the following time points : UPN01: day 15; UPN03: day 15; UPN 07: day 43; UPN08: day 29; UPN09: day 15 (middle circle) and day 29 (inner circle); UPN10 (day 29). Z-scores >1·5 (suggesting gain) are shown in blue, and z-scores < -1·5 (suggesting loss) in red, where darker colors represent higher absolute values of z-scores. Z-scores between -1·5 and +1·5 are shown in yellow. Seven color grades are used to indicate six z-score intervals of length 0.75 ranging from 1·5 (-1·5) to 6 (-6). The seventh, darkest color is reserved for values >6 or <-6.

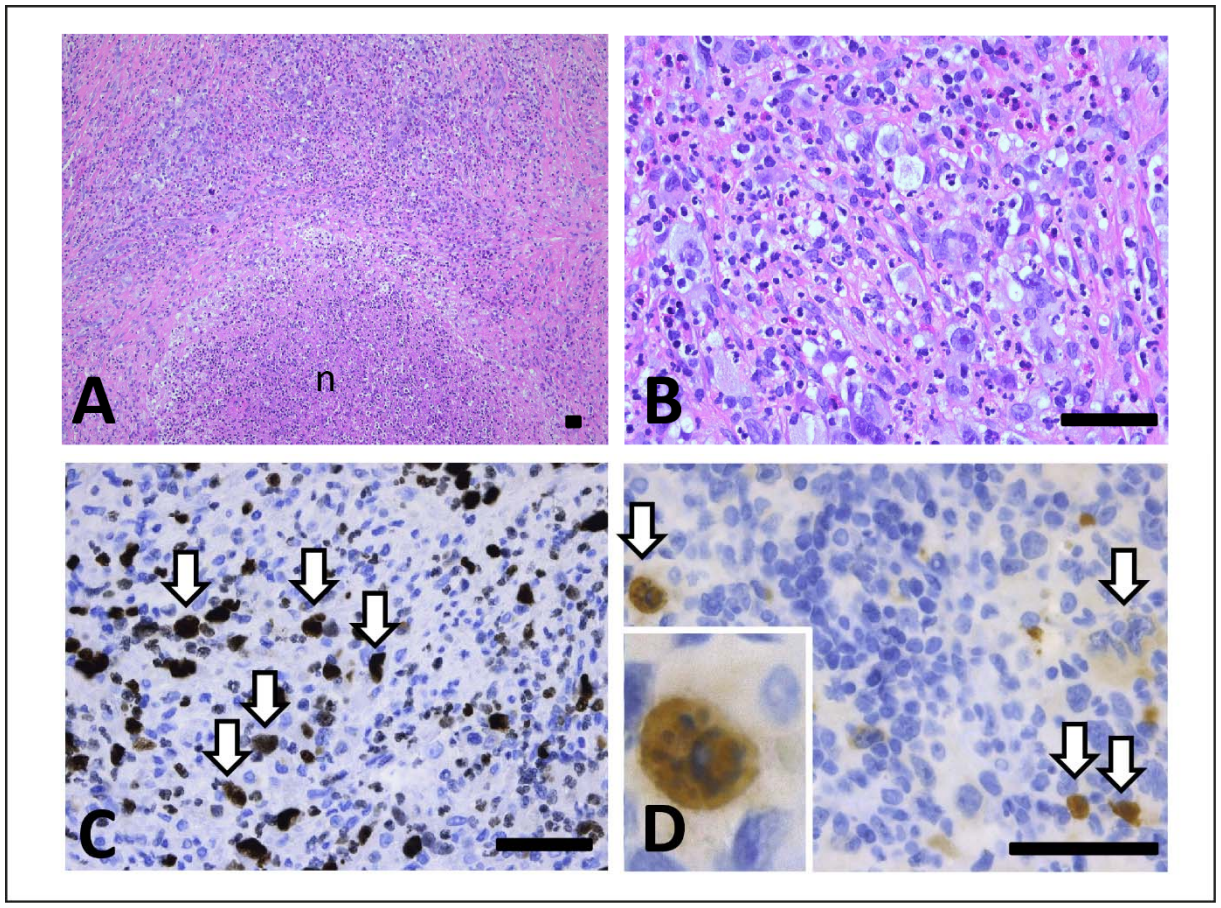

Figure 5. **Areas of necrosis, expression of Ki67 and presence of cleaved caspase-3 in NS Hodgkin's lymphoma.**

A. Low power view of architectural effacement of lymph node involved by classical Hodgkin lymphoma, including areas of necrosis (n) (Hematoxylin Eosin);

B. High power view of neoplastic Hodgkin/Reed-Sternberg-cells in a background of non-neoplastic stromal cells, containing lymphocytes, eosinophils, neutrophils, plasmacells and histiocytes (Hematoxylin Eosin).

C. Hodgkin/Reed-Sternberg-cells show a high proliferation index (anti-Ki67/Mib1 immunostaining);

D. Hodgkin/Reed-Sternberg-cells show signs of apoptosis, with karyorrhexis (see inset) and/or cytoplasmic expression of cleaved Caspase-3 (anti-cleaved caspase-3 HRP immunostaining); Arrows indicate Hodgkin/Reed Sternberg cells (Hodgkin/Reed-Sternberg); scalebar: 50µm

TABLE 1

				Recurrent imbalances suggested by GR profiling and validated by interphase FISH											
				2p			7q			9p/9pter			other		
				GR[b]	FISH[c]	concordant [d]	GR[b]	FISH[c]	concordant [d]	GR[b]	FISH[c]	concordant [d]	GR[b]	FISH[c]	con
Case	Sex/ age (y)	Stage	Cytogenetics[a]		*ALK* (2p23) #signals[#cells]			*D7S486* (7q31) /CEP7 #signals[#cells]			*JAK2* (9p24) /CEP8 #signals[#cells]			probe (region): #signals[#cells]	
UPN01	F/27	IIA	ND	normal	ND	-	normal	ND	-	gain	amp/2[11]	Y	8qter gain chr.14 gain	*MYC* (8q24): 3-6[7] *IGH@* (14q32): 4-5[7]	
UPN02	F/65	IIA	NM	normal	2[2]	Y	normal	ND	-	normal	2/2[3]	Y		-	
UPN03	F/21	IIA	ND	gain	2[2]; 4[4]; 5[1]; 13[1]	Y	loss	2/4[1]; 3/6[1]; 5/6[1]	Y	gain	4/2[1]; 5/2[1]; 6/1-3[3]; 7/1-4[2]; 8/2-3[2]; 9/2[1]	Y		-	
UPN04	F/12	IIA	NM	gain	2[1]; 6[1], 8[2],amp[7]	Y	loss	3/4[2]; 3/5[3]; 5/7[2]; 7/8[1]	Y	gain 9p/ normal 9p24	4/2[1]; 4/4[1]; 6/2[1]; 6/4[3]; 7/2[1]; 8/5[1]	N		-	
UPN05	F/17	IIA	abnormal	gain	4[4]; 5[5]	Y	normal	4/4[10]	Y	loss ?	2/3[9]	Y			
UPN06	F/18	IIA	abnormal	normal	4[3]	N	normal	ND	-	gain	5/3[3]; 5/4[1]; 7/3[2]	Y			
UN07	M/30	IIA	46,XY[1]	gain	3[1]; 4[2]; 5[3]; 7[1]; 8[1]; 13[1]	Y	normal	ND	-	gain	9/4[1]; 9/5[1]; 10/5[1]; 10/7[1]; 11/5[1]	Y		-	
UPN08	M/26	IVB	46,XY[3]	gain	5[2]; 6[3]; 7[1]; 10[1]; >10[1]	Y	loss	2/4[1]; 4/8[1]	Y	gain 9p/ normal 9p24	2/2[1]; 3/3[2]; 5/3[1]; 7/3[1]; 7/6[1]	P	1q gain 7p gain	*CKS1B* (1q21)/CEP1: 3/2[3]; 6/4[1] *TCRG@* (7p14)/CEP7: 4/3[3]	
UPN09	M/39	IVEB	NM	gain	5[1]; 6[2]; 7+amp[1]	Y	loss	1/2[1]; 1/4[1]; 3/4[1]; 3/5[1]; 5/7[1]; 6/9[1]; 8/15[1]	Y	normal	3/4[1]; 4/4[1]; 5/3[1]; 6/9[1]	P			
UPN10	F/45	IIA	46,XX[20]	gain	4[12]; 5[1]; 8[1]; 10[1]	Y	loss	2/3[5]	Y	loss	3/3[7]; 6/4[1];9/5[1]	N			

[a] Cytogenetics : in case UPN05 and 06, one and two abnormal metaphases were identified respectively, indicating a pseudotriploid status of the Hodgkin/Reed-Sternberg cell. ND: not done. NM: no metaphases

[b] Status of the indicated region as analyzed by genomic representation profiling

[c] FISH was performed with the probes indicated. Giant Hodgkin/Reed-Sternberg cells were evaluated. Hybridization patterns of Hodgkin/Reed-Sternberg cells are shown, followed by the number of Hodgkin/Reed-Sternberg cells with the given pattern between square brackets. Different hybridization patterns are separated by ";". ND: not done

[d] Concordance between FISH and genomic representation profiling. Y: yes. N: no. P: partial

RESEARCH IN CONTEXT

Systematic review :

We searched PubMed for articles on cell-free DNA and Hodgkin lymphoma or non-Hodgkin lymphoma, excluding Epstein-Barr virus. This retrieved only two articles indicating that increased levels of circulating cell-free DNA can be found in non-Hodgkin and Hodgkin lymphoma, and correlate with adverse features. Whether this circulating cell-free DNA originated from malignant versus non-malignant cells was not investigated.

We also searched PubMed for articles with “Hodgkin lymphoma” and “genome, genetics, mutations, chromosome or cytogenetics” (in the title or abstract), excluding non-Hodgkin lymphoma and Nodular lymphocyte predominant Hodgkin Lymphoma. This search retrieved 35-45 relevant research articles published between 1993 and present. These papers studied either Hodgkin Lymphoma derived cell-lines, cultured cells from Hodgkin Lymphoma biopsies, Hodgkin/Reed-Sternberg cells identified by immunohistochemistry in biopsies, or Hodgkin-Reed/Sternberg cells purified by laser microdissection or flow cytometry from Hodgkin Lymphoma biopsies. The methods used were cytogenetics, FICTION (a combination of FISH and immunohistochemistry), array comparative genomic hybridization, gene-expression profiling or mutational analysis.

Interpretation

This is the first report that genetic features of Hodgkin/Reed-Sternberg cells in classical Hodgkin Lymphoma can be revealed by analysis of cell-free circulating DNA. Given the technical difficulty to analyse the genetics of primary Hodgkin/Reed-Sternberg cells in biopsies, analysis of circulating cell-free DNA may open up new translational avenues for the development of biomarkers and of precision medicine in classical Hodgkin lymphoma.